Experimental Gerontology 104 (2018) 127–137

Contents lists available at ScienceDirect

Experimental Gerontology

journal homepage: www.elsevier.com/locate/expgero

Differential response to caloric restriction of retroperitoneal, epididymal, and subcutaneous adipose tissue depots in rats

Takumi Narita[a,b,1], Masaki Kobayashi[a,b,1], Kaho Itakura[a], Rei Itagawa[a], Riho Kabaya[a], Yuka Sudo[b], Naoyuki Okita[b,c], Yoshikazu Higami[a,b,*]

[a] Molecular Pathology and Metabolic Disease, Faculty of Pharmaceutical Sciences, Tokyo University of Science, Noda, Japan
[b] Translational Research Center, Research Institute of Science and Technology, Tokyo University of Science, Noda, Japan
[c] Department of Internal Medicine Research, Sasaki Institute, Sasaki Foundation, Tokyo, Japan

ARTICLE INFO

Section Editor: Holly M. Brown-Borg

Keywords:
Caloric restriction
White adipose tissue
Lipid metabolism
Insulin signaling
Macrophage

ABSTRACT

The beneficial actions of caloric restriction (CR) are partially mediated by metabolic remodeling of white adipose tissue (WAT). Recently, we showed that CR enhances de novo fatty acid (FA) biosynthesis and mitochondrial biogenesis, particularly in WAT. Here, to better understand the response of WAT to CR, we compare the effects of CR on three WAT depots in rats: retroperitoneal (rWAT), epididymal (eWAT) and subcutaneous (sWAT). Computed tomography and histological analysis showed that CR reduced the volume and average size of rWAT adipocytes. In all WAT depots, CR markedly upregulated the expression of proteins involved in FA biosynthesis in fed rats. In visceral WAT (rWAT and eWAT), hormone-sensitive lipase (lipolytic form) phosphorylation was increased by CR under fed conditions, and decreased by CR under fasted conditions. Conversely, in sWAT, hormone-sensitive lipase phosphorylation was increased by CR under fasted conditions. CR enhanced the effect of feeding on AKT activity in sWAT (indicative of a positive effect on insulin sensitivity) but not in rWAT or eWAT. These data suggest that CR improves lipid metabolism in an insulin signaling-dependent manner in sWAT only. The effects of CR on adipokine (adiponectin and leptin) expression were also different among rWAT, eWAT and sWAT, and CR reduced the gene expression of M2 macrophage markers in rWAT and sWAT, but not in eWAT. We conclude that CR differentially affects the characteristics of WAT depots in rats, including adipocyte size, lipid metabolism, insulin signaling, adipocytokine profile and macrophage infiltration.

1. Introduction

White adipose tissue (WAT) is a major site of energy storage in the form of triglycerides (TG), and consists predominantly of adipocytes containing unilocular lipid droplets. However, it is now clear that WAT is also a major endocrine organ. Several WAT-secreted molecules, known as adipocytokines, have been characterized, whose secretory profiles are modified according to adipocyte size. Hypertrophic adipocytes, which contain more TG, secrete less adiponectin, fewer anti-inflammatory and anti-atherogenic cytokines, and more proinflammatory adipokines, including leptin and monocyte chemotactic protein 1. In contrast, small adipocytes secrete more adiponectin and smaller amounts of proinflammatory adipokines (DeClercq et al., 2008; Torres-Leal et al., 2010; Ouchi et al., 2011).

Caloric restriction (CR) is the most robust, reproducible, and simple experimental manipulation known to extend lifespan and delay onset of many age-associated pathophysiological changes in laboratory rodents. We previously reported that CR upregulates expression of sterol regulatory element-binding protein-1c (Srebp-1c), a master transcriptional regulator of proteins involved in fatty acid (FA) biosynthesis, and its downstream target genes, in a growth hormone/insulin-like growth factor-independent manner (Chujo et al., 2013). In fact, previous reports have shown that CR-enhanced de novo FA biosynthesis occurs predominantly in WAT, rather than in liver (Bruss et al., 2010). We have also shown that CR significantly upregulates the expression of proteins involved de novo FA biosynthesis and mitochondrial biogenesis in WAT in an Srebp-1c-dependent manner, but does not in the other tissues (Okita et al., 2012; Fujii et al., 2017). Therefore, we consider that metabolic remodeling of WAT plays a very important role in the beneficial actions of CR. Moreover, it takes more than three months to

* Corresponding author at: Molecular Pathology and Metabolic Disease, Faculty of Pharmaceutical Sciences, Tokyo University of Science, 2641 Yamazaki, Noda, Chiba 278-8510, Japan.
E-mail addresses: 3B15706@ed.tus.ac.jp (T. Narita), kobayashim@rs.tus.ac.jp (M. Kobayashi), 3B14610@ed.tus.ac.jp (K. Itakura), 3B17605@ed.tus.ac.jp (R. Itagawa), j3a12030@ed.tus.ac.jp (R. Kabaya), ysudo@rs.tus.ac.jp (Y. Sudo), nmsokita@gmail.com (N. Okita), higami@rs.noda.tus.ac.jp (Y. Higami).
[1] These authors contributed equally to the work.

https://doi.org/10.1016/j.exger.2018.01.016
Received 17 July 2017; Received in revised form 13 January 2018; Accepted 15 January 2018
Available online 02 February 2018

Table 1
Body and tissue weight, and plasma parameter.

Body and tissue weight		AL		CR		*p* Values (2-way ANOVA)		
		Fed	Fast	Fed	Fast	Fed/fast effect	AL/CR effect	Interaction effect
Body weight	(g)	529.84 ± 12.38	532.11 ± 21.00	396.49 ± 16.76***	364.27 ± 11.23***	0.3553	< 0.0001	0.2887
rWAT	(g)	8.75 ± 0.71	8.51 ± 0.66	1.84 ± 0.21***	1.83 ± 0.36***	0.8123	< 0.0001	0.8232
eWAT	(g)	7.93 ± 0.62	8.25 ± 0.69	2.85 ± 0.16***	2.82 ± 0.20***	0.7604	< 0.0001	0.7178
sWAT	(g)	9.80 ± 0.71	8.62 ± 1.51	2.58 ± 0.39***	2.01 ± 0.26***	0.3237	< 0.0001	0.7328
BAT	(g)	0.41 ± 0.06	0.34 ± 0.01	0.27 ± 0.03*	0.18 ± 0.02*	0.0350	0.0003	0.7339
Heart	(g)	1.29 ± 0.05	1.40 ± 0.06	1.07 ± 0.03*	1.02 ± 0.03***	0.5550	< 0.0001	0.0717
Liver	(g)	19.22 ± 0.73	15.96 ± 0.58 $$	18.75 ± 0.57	10.87 ± 0.35***$$$	< 0.0001	0.0001	0.0006
Spleen	(g)	0.88 ± 0.03	0.91 ± 0.06	0.71 ± 0.03*	0.69 ± 0.03**	0.9786	0.0001	0.5638
Kidney	(g)	1.74 ± 0.06	1.70 ± 0.06	1.21 ± 0.07***	1.20 ± 0.04***	0.7153	< 0.0001	0.8974
Plasma parameter								
Glucose	(mg/dL)	762.07 ± 60.92	549.12 ± 58.34	428.61 ± 28.95**	467.09 ± 94.76	0.1950	0.0046	0.0676
Insulin	(pg/mL)	1549.76 ± 232.22	477.25 ± 91.87 $$$	1787.84 ± 102.61	224.56 ± 22.10 $$$	< 0.0001	0.9575	0.0851
Adiponectin	(ng/mL)	769.26 ± 64.68	596.09 ± 56.02	980.45 ± 72.73	964.36 ± 60.69**	0.1537	0.0002	0.2328

	CR/AL	
	Fed	Fast
Body weight	0.748	0.685
rWAT	0.210	0.215
eWAT	0.359	0.342
sWAT	0.264	0.233
BAT	0.664	0.532
Heart	0.831	0.724
Liver	0.976	0.681
Spleen	0.804	0.757
Kidney	0.698	0.702

Each value represents the means ± S.E.M. of 6 mice. *: $p < 0.05$, **: $p < 0.01$, ***: $p < 0.001$ vs. AL, $$: $p < 0.01$, $$$: $p < 0.001$ vs. fed, analyzed by Tukey's test.
WAT: white adipose tissue, eWAT: epididymal WAT, rWAT: retroperitoneal WAT, sWAT: subcutaneous WAT, BAT: brown adipose tissue.

complete the beneficial metabolic remodeling that is induced by CR, including enhancement of de novo FA synthesis in WAT (Okita et al., 2015). It is well known that ATP citrate lyase (ACLY) and malic enzyme 1 (ME-1) are major proteins involved in de novo FA biosynthesis. ACLY is the cytosolic enzyme that converts citrate into acetyl-coenzyme A, a substrate of FA biosynthesis. ME-1 is the cytosolic NADP-dependent enzyme that generates NADPH, a coenzyme of FA biosynthesis, by converting malate into pyruvate (Strable and Ntambi, 2010).

WAT is distributed throughout the body, but each depot has specific characteristics. For example, it is known that lipolytic activity and FA turnover are more readily activated in visceral WAT (vWAT) than in subcutaneous WAT (sWAT) (Engfeldt and Arner, 1988). In addition, in humans, the expression of adiponectin and leptin is lower in vWAT than in sWAT (Fisher et al., 2002). These differences are considered to be involved in the divergence in metabolic syndrome risk between viscerally obese and subcutaneously obese patients. It has been reported that in mice, transplantation of sWAT into the visceral compartment reduces body weight, fat mass, plasma glucose and insulin levels, and improves insulin sensitivity. These findings suggest that sWAT is intrinsically different from vWAT (Tran et al., 2008).

In this study, we aimed to characterize the response of WAT to CR in greater detail by comparing the effects of six months of CR on vWAT (retroperitoneal WAT [rWAT] and epididymal WAT [eWAT]) and sWAT in rats.

2. Material and methods

2.1. Animals and diet

The present study was approved by the Ethics Review Committee for Animal Experimentation at the Tokyo University of Science. Male 5–7-week-old Wistar rats were purchased from Clea Inc. (Tokyo, Japan) and maintained under specific pathogen-free conditions in the Laboratory Animal Center in the Faculty of Pharmaceutical Sciences, Tokyo University of Science. The animals, their husbandry, and diet have been previously described in detail (Okita et al., 2012).

All rats were provided with water and fed ad libitum with a Charles River Formula-1 diet (Oriental Yeast, Japan). At 12 weeks of age, the rats were divided into two groups: one was fed ad libitum (AL group) and the other was calorie restricted (CR group; 70% of AL energy intake). At 9 months of age, rats were euthanized under isoflurane anesthesia (Mylan, Canonsburg, PA, USA) 3–5 h after the lights came on. Prior to euthanasia, CR and AL groups were further divided into fed and fasted subgroups. Half of the CR rats were provided with food 30 min prior to the lights going off in the evening, and were euthanized the following morning (CR-fed), while the other half were fasted for ~24 h before euthanasia (CR-fast). Similarly, half of the AL rats were euthanized without first removing their food (AL-fed), while the other half were euthanized ~20 h after their food was removed, at the time the lights went off (AL-fast). When they were euthanized, the retroperitoneal, epididymal and subcutaneous WAT depots were dissected, and their masses, and the total body mass, were measured. Thereafter, the tissues were immediately diced, frozen in liquid nitrogen, and stored at −80 °C. A subsample of each WAT depot was fixed in buffered formalin solution for subsequent histological examination.

2.2. Computed tomography

We validated a computed tomography (CT) method using the third-generation CT scanner, LaTheta LCT-200 (Hitachi-Aloka, Tokyo, Japan). The tube voltage was set to 50 kV and the current was constant at 0.5 mA. Animals were scanned in a 120 mm-wide specimen holder with a resolution of 96 μm per pixel. For all scans the same number of views (436) was used, which was the number of data points collected

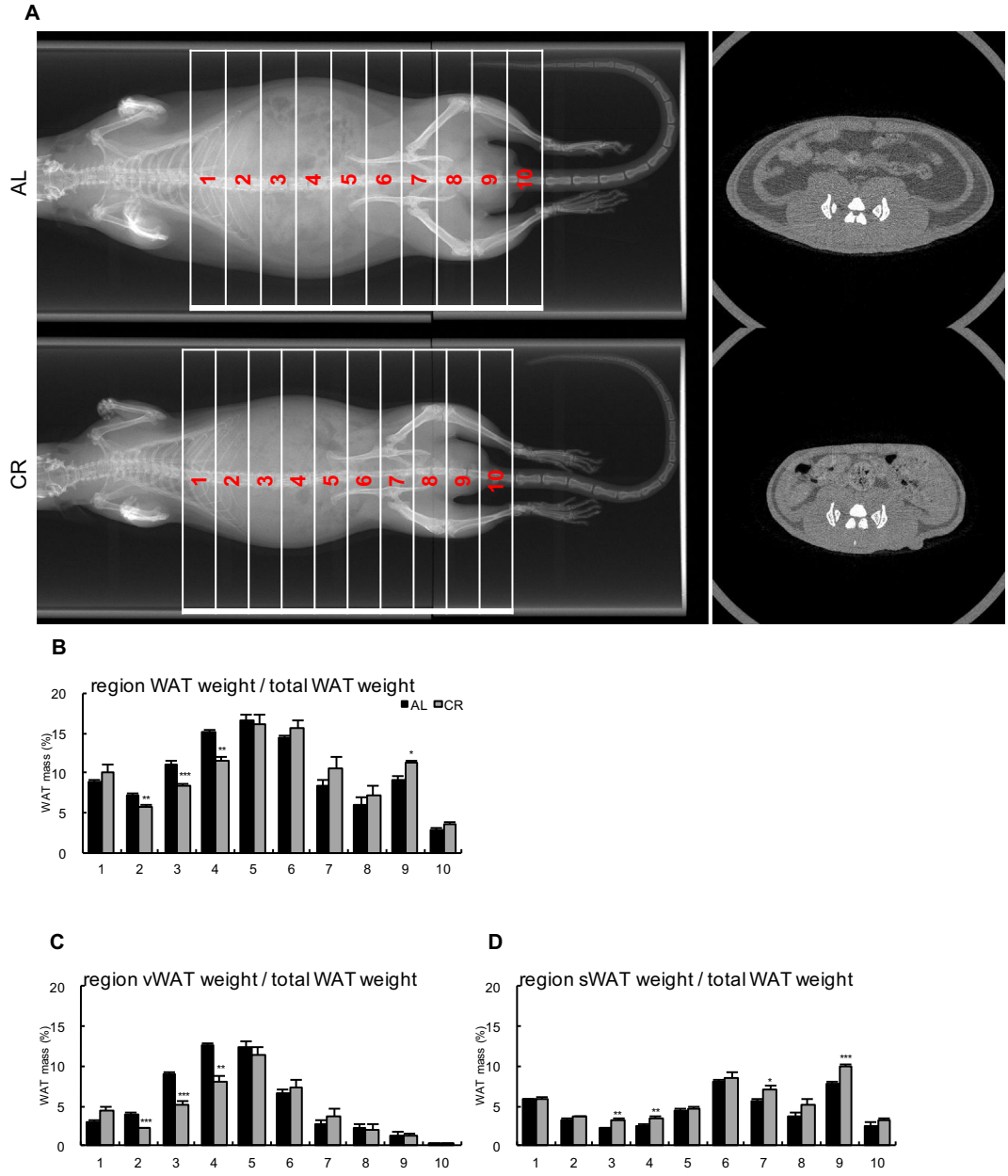

Fig. 1. Body fat distribution
WAT depot size per whole slice was determined by CT scan. (A) Whole body X-ray image, (B) Regional WAT volume/total WAT volume, (C) Regional vWAT volume/total WAT volume, and (D) Regional sWAT volume/total WAT volume. Error bars represent SEM ($n = 4$). CT image slices were taken from section 10, described in (A). *: $p < 0.05$, **: $p < 0.01$, ***: $p < 0.001$ vs AL, analyzed by Student's *t*-test.

during a single 360° rotation around the object. In accordance with the manufacturer's recommendations, the estimated radiation exposure of the rats was kept below 40 mSv. In pilot experiments, optimal scanning conditions were evaluated for each tissue and the final conditions were set at a −550 to −140 Hounsfield unit density range, 240 μm slice thickness, and a 1500 μm slice pitch. vWAT and sWAT were distinguished according to whether they were located inside (visceral) or outside (subcutaneous) of body wall muscles such as the abdominal and thoracic wall muscles.

2.3. Histological examination

WAT was fixed in buffered 10% formalin solution, processed routinely, embedded in paraffin, cut into 5 μm sections, and stained with hematoxylin and eosin. The stained sections were scanned under a microscope, using a charge-coupled device camera (Nikon, Tokyo, Japan). The size distribution of the white areas in the black and white images, representing lipid droplets, was evaluated using ImageJ 1.43u/Java1.6.0_22 software (http://rsbweb.nih.gov/ij/). To avoid inter-individual variation, a single observer carried out the morphometric analysis.

2.4. Plasma biochemical analysis

Plasma glucose, insulin, and adiponectin were measured by LabAssay Glucose (Wako, Osaka, Japan), Rat Insulin ELISA Kit (U-E type) (Shibayagi, Gunma, Japan), and Mouse/Rat High Molecular Weight Adiponectin ELISA KIT (Shibayagi), respectively. All assays were performed according to the manufacturers' protocols.

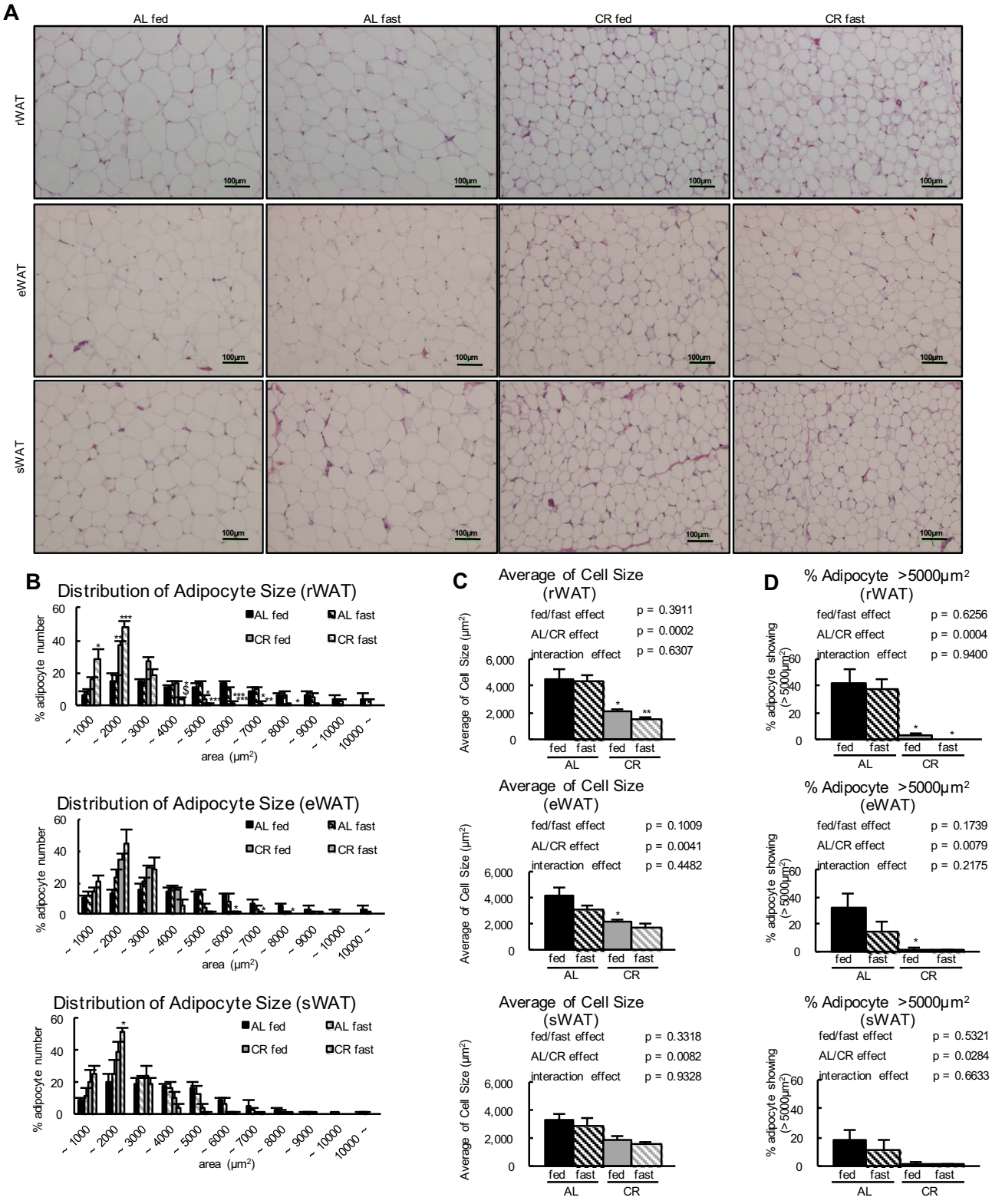

Fig. 2. Histology of rWAT, eWAT and sWAT in AL and CR rats

(A) Representative histological sections of rWAT, eWAT and sWAT from AL and CR rats (magnification: ×100, scale bar: 100 μm). Sections were stained with hematoxylin and eosin. (B) Distribution of adipocyte size in rWAT, eWAT and sWAT, measured using a quantitative morphometric method in ImageJ 1.43 μ/Java1.6.0_22 software. (C) Mean adipocyte size, and (D) Percentage of large adipocytes (> 5000 μm²) in rWAT, eWAT and sWAT. Values are mean ± SEM ($n = 6$). *: $p < 0.05$, **: $p < 0.01$ vs AL, $: $p < 0.05$ vs. fed, analyzed by Tukey's test after 2-way ANOVA.

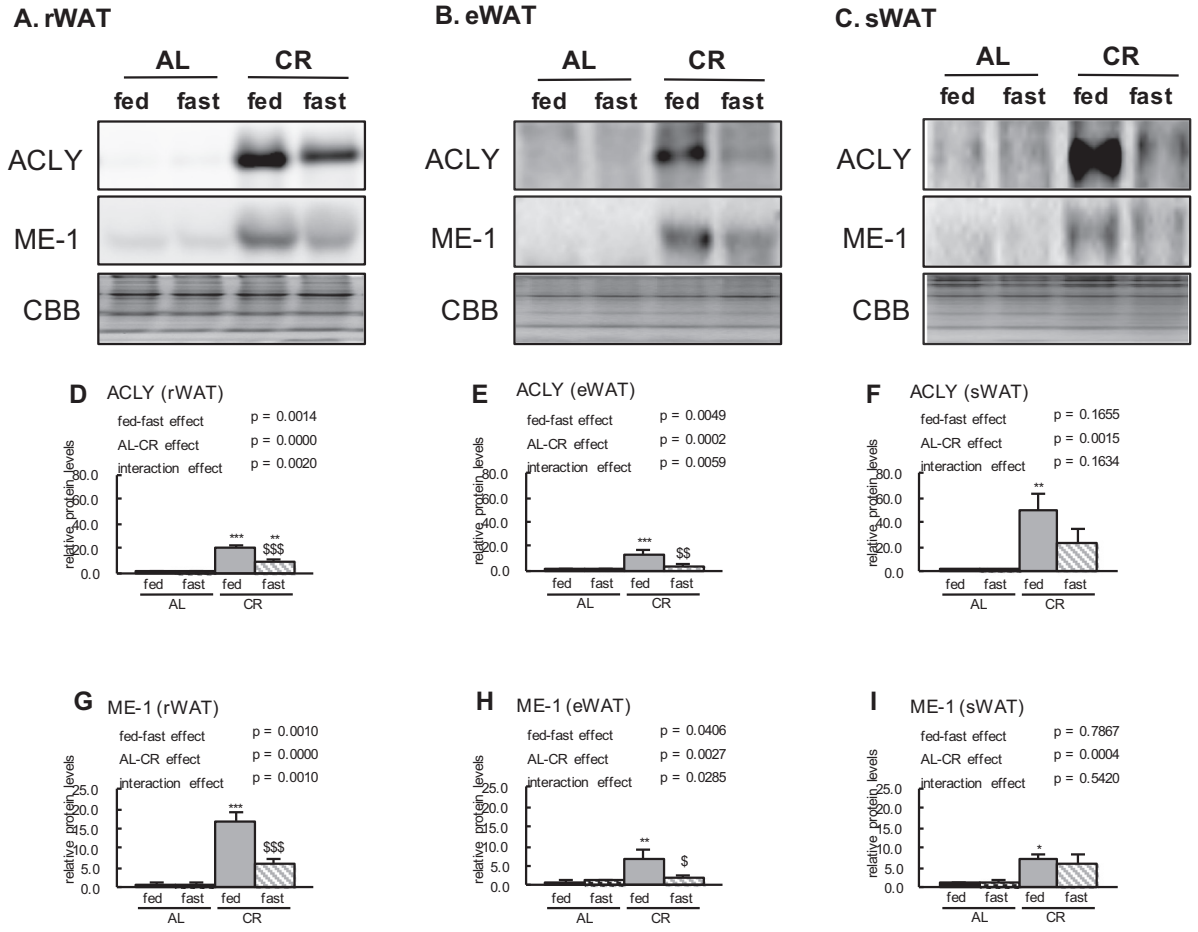

Fig. 3. Expression of proteins involved in lipogenesis in rWAT, eWAT and sWAT

Sample immunoblot images showing expression of proteins involved in lipogenesis in rWAT (A), eWAT (B), and sWAT (C) from the four groups (AL-fed, AL-fast, CR-fed, CR-fast). Quantitative analysis of immunoblots was performed using a chemiluminescence method. Results for total ACLY (D–F) and ME-1 (G–I) are expressed as relative intensity of the indicated protein/Coomassie Brilliant Blue staining, compared with values in the AL-fed group (n = 5–6 per group). Values are mean SEM *: $p < 0.05$, **: $p < 0.01$, ***: $p < 0.001$ vs. AL, $: $p < 0.05$, $$: $p < 0.01$, $$$: $p < 0.001$ vs. fed, analyzed by Tukey's test after 2-way ANOVA.

2.5. Protein extraction and western blotting analysis of target protein abundance

WAT samples were lysed in lysis buffer (50 mM Tris–HCl pH 6.8, 2% SDS, 3 M urea, 6% glycerol) by boiling for 5 min followed by sonication. Lysate protein concentrations were determined using a BCA Protein Assay Kit (Thermo Fisher Scientific, Rockford, IL, USA), and their concentrations normalized. Next, 2-mercaptoethanol and bromophenol blue were added to the protein samples to final concentrations of 5% and 0.025%, respectively, and the samples were boiled for 5 min. Equal amounts of protein (5–20 μg) were subjected to SDS-PAGE and transferred to nitrocellulose membranes. The membranes were blocked with 2.5% skim milk and 0.25% bovine serum albumin in Tris-buffered saline (50 mM Tris–HCl pH 7.4, 150 mM NaCl) containing 0.1% Tween-20 (TTBS) for 1 h at room temperature, and then probed with appropriate primary antibodies overnight at 4 °C, or for 2 h at room temperature. The primary antibodies used targeted ACLY (Epitomics, Burlingame, CA, USA), malic enzyme 1 (ME-1) (Sigma-Aldrich Co., Darmstadt, Germany), hormone sensitive lipase (HSL) (Cell Signaling, Boston, MA, USA), phosphorylated HSL (Ser563) (pHSL) (Cell Signaling), adipose triglyceride lipase (ATGL) (Cell Signaling), total insulin receptor substrate-1 (IRS1) (Merck, Darmstadt, Germany), total AKT (AKT) (Cell Signaling), and phosphorylated AKT (pAKT; Ser473) (Cell Signaling). After washing with TTBS, the membranes were incubated with an appropriate secondary antibody (horseradish peroxidase-conjugated F(ab′)2 fragment of goat anti-mouse IgG or anti-rabbit IgG [Jackson Immuno Research, West Grove, PA, USA]), for 1 h at room temperature. After washing with TTBS, the membranes were incubated with ImmunoStar LD Reagent (Wako). The antibody-bound proteins were visualized with an LAS3000 Image Analyzer (Fujifilm, Tokyo, Japan), and data were analyzed using Multigauge software (Fujifilm).

2.6. RNA extraction and real-time RT-PCR

Total RNA was extracted from frozen WAT using the ReliaPrep RNA Tissue Miniprep System (Promega, Tokyo, Japan), in accordance with the manufacturer's protocol. To obtain cDNA, 1 μg of RNA was subjected to reverse transcription using PrimeScript Reverse Transcriptase (Takara, Shiga, Japan) and random hexamer primers (Takara). Real-time quantitative PCR was performed using a CFX connect Real-time PCR System (Bio−Rad, Hercules, CA, USA) and Thunderbird SYBR qPCR Mix (Toyobo, Osaka, Japan) according to the manufacturers' protocols. Transcripts of *Adiponectin*, *Leptin*, *F4/80*, *Cd11c*, *Cd163*, *Il-6*, *Tnfa* and *TATA box-binding protein* (*Tbp*) were amplified, with *Tbp* being used for normalization. The primer sequences are shown in Table S1.

2.7. Statistical analysis

Data are presented as mean ± standard error of the mean (SEM). Statistical significance was determined using Student's *t*-test for two groups, or Tukey's test after 2-way ANOVA for the comparison of more than two groups.

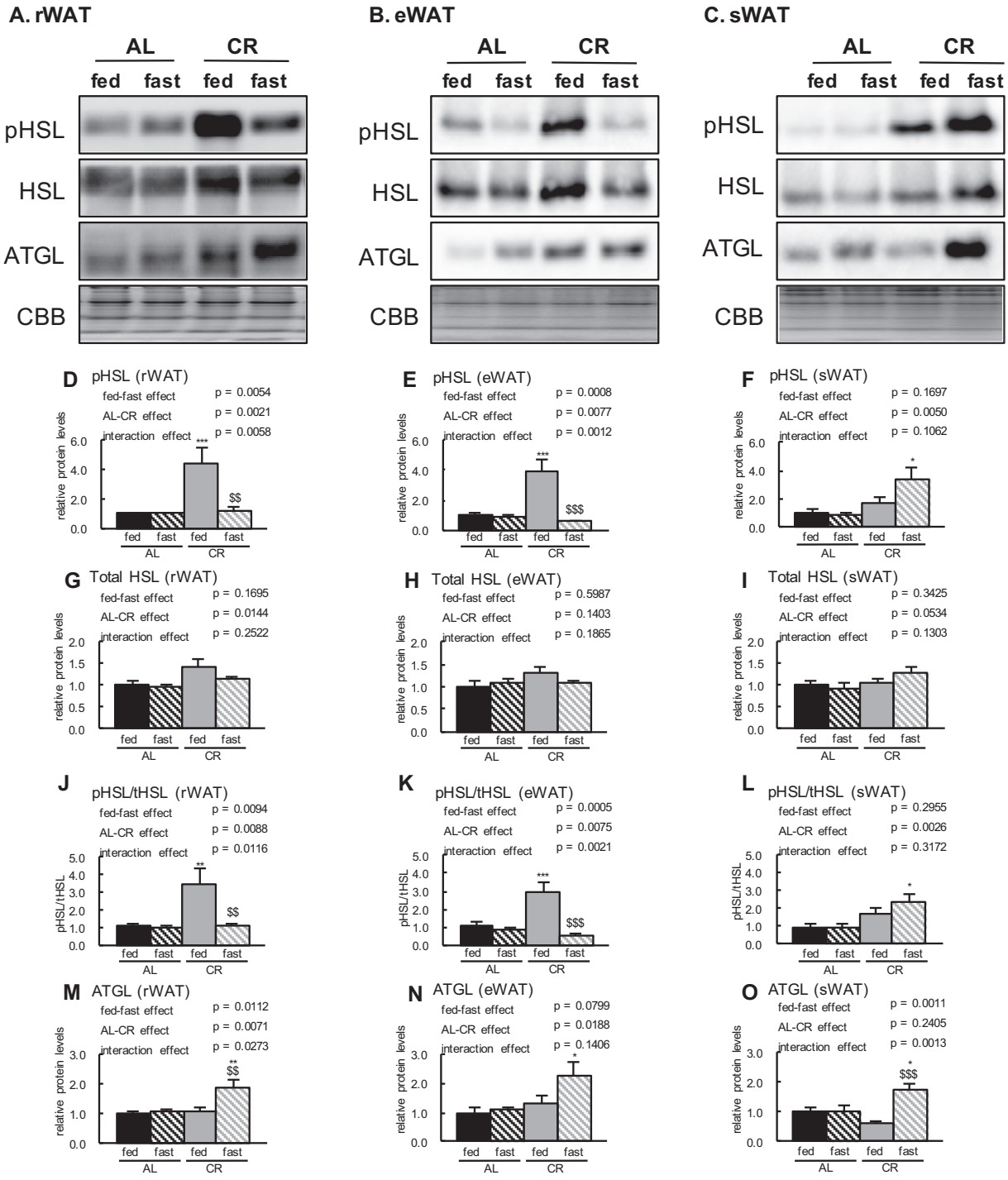

Fig. 4. Expression of proteins involved in lipolysis in rWAT, eWAT and sWAT

Sample immunoblot images showing expression of proteins involved in lipolysis in rWAT (A), eWAT (B), and sWAT (C), in the four groups (AL-fed, AL-fast, CR-fed, CR-fast). Quantitative analysis of immunoblots was performed using a chemiluminescence method. Results for pHSL (D–F), total HSL (G–I), pHSL/total HSL (J–L) and ATGL (M–O) are expressed as relative intensity of the indicated protein/CBB staining, compared with values in the AL-fed group (n = 5–6 per group). Values are mean ± SEM *: $p < 0.05$, **: $p < 0.01$, ***: $p < 0.001$ vs. AL, $$: $p < 0.01$, $$$: $p < 0.001$ vs. fed, analyzed by Tukey's test after 2-way ANOVA.

3. Results

3.1. Adipose depot mass and volume

Body and WAT masses, particularly rWAT mass, were significantly lower in CR rats (Table 1). Therefore, we analyzed the distribution of WAT in detail, using CT images that allowed us to calculate the volume of 10 regions of WAT mass, separate from the diaphragm and testes (Fig. 1A). The ratio of WAT depot volume to total WAT volume in CR rats was significantly lower in regions 2–4, and higher in region 9 (Fig. 1B). To further evaluate this altered distribution, we distinguished between vWAT and sWAT. This showed that in CR rats, the ratio of vWAT volume to total WAT volume was significantly lower in regions 2–4, and the ratio of sWAT volume to total WAT volume was significantly higher in regions 3, 4, 7 and 9, and tended to be higher in region 8 (Fig. 1C and D). These observations suggest that CR reduces

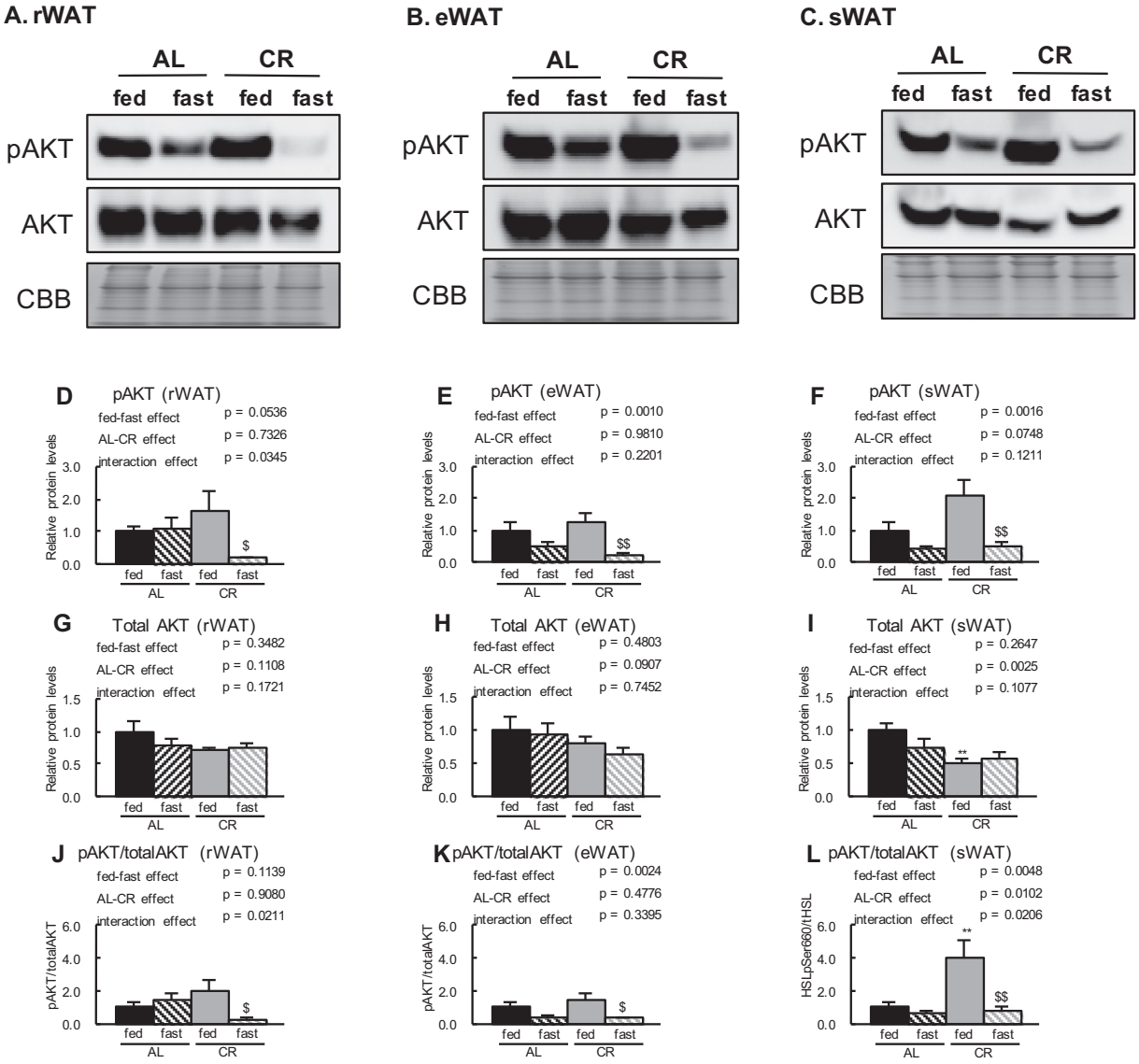

Fig. 5. Expression of proteins involved in insulin signaling in rWAT, eWAT and sWAT

Sample immunoblot images showing expression of proteins involved in insulin signaling in rWAT (A), eWAT (B), and sWAT (C), from the four groups (AL-fed, AL-fast, CR-fed, CR-fast). Quantitative analysis of immunoblots was performed using a chemiluminescence method. Results for pAKT (D–F), total AKT (G–I), and pAKT/total AKT (J–L) are expressed as relative intensity of the indicated protein/CBB staining, compared with values in the AL-fed group (n = 5–6 per group). Values are mean ± SEM **: $p < 0.01$ vs. AL, $: $p < 0.05$, $$: $p < 0.01$ vs. fed, analyzed by Tukey's test after 2-way ANOVA.

vWAT volume—particularly rWAT volume—rather than sWAT volume.

3.2. Histological analysis

Next, we compared adipocyte size distribution among the three WAT depots histologically. The adipocytes appeared larger in rWAT and smaller in sWAT than in eWAT. By 2-way ANOVA analysis, CR markedly reduced the average size of the adipocytes and the percentage of large adipocytes ($> 5000\ \mu m^2$) in the three WAT depots (Fig. 2A–D). By Tukey's test, this CR effect was statistically significant in both rWAT and eWAT of fed rats, whereas, under fasting conditions, only rWAT showed a significant reduction. In contrast, CR did not significantly reduce adipocyte size in sWAT of fed or fasted rats. These results suggest that CR reduced adipocyte size, but that this effect might be greater in rWAT than eWAT, and negligible in sWAT.

3.3. Expression of proteins involved in fatty acid biosynthesis and lipolysis in the three WAT depots

We previously reported that CR upregulated the expression of proteins involved in FA biosynthesis in eWAT (Okita et al., 2015). We measured ACLY and ME-1 protein abundance in the three WAT depots, and found that CR markedly and similarly upregulated their abundance in all three depots (Fig. 3). However, ACLY and ME-1 abundance was downregulated under fasting conditions compared with fed conditions in CR rats in rWAT and eWAT, but not in sWAT (Fig. 3). We also measured the abundance of the lipolytic proteins HSL, active pHSL, and ATGL. HSL abundance was markedly upregulated by CR in rWAT and sWAT, but not in eWAT (Fig. 4A–C, G–I). pHSL abundance was also significantly upregulated by CR in all three WAT depots, but this CR-associated upregulation was attenuated in rWAT and eWAT after fasting (Fig. 4A–F, J–L). ATGL abundance was significantly upregulated by CR in rWAT and sWAT of fasted rats, and tended to be upregulated by CR in eWAT of fasted rats (Fig. 4A–C, M–O). These results suggest that the effects of CR on lipolytic proteins are different between vWAT

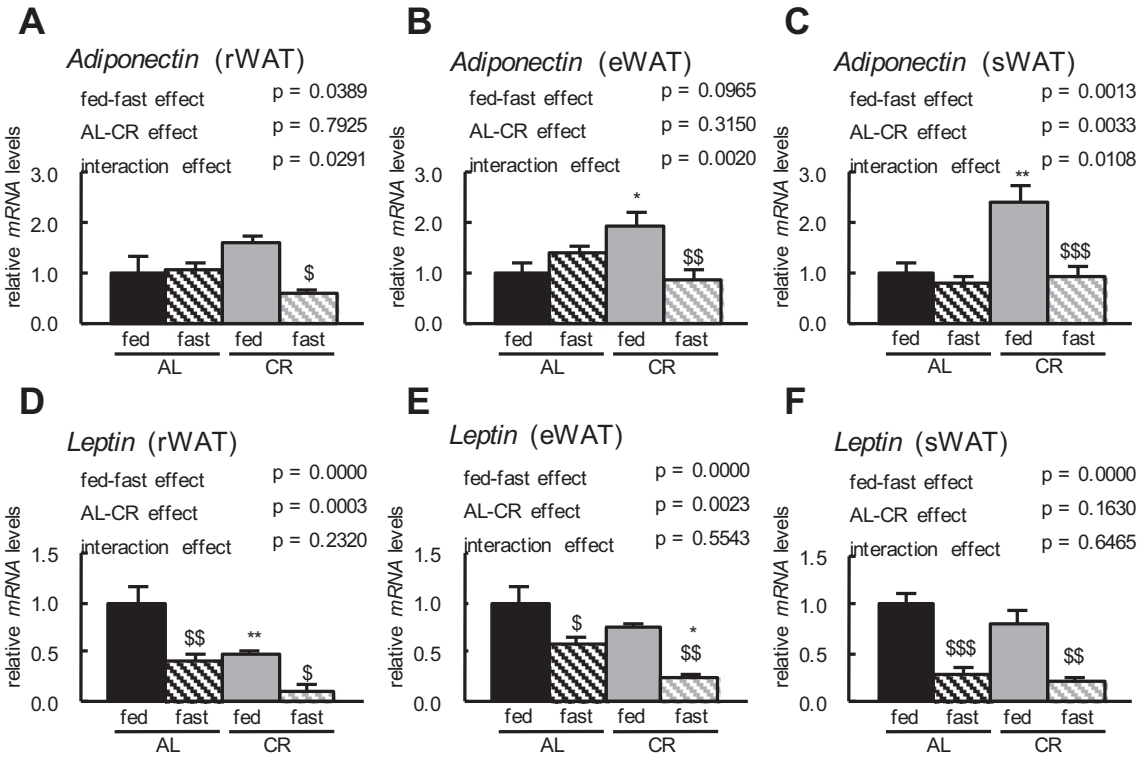

Fig. 6. Expression of adipocytokine genes in rWAT, eWAT and sWAT

mRNA expression of adiponectin (A–C) and leptin (D–F), in rWAT, eWAT and sWAT from the four groups (AL-fed, AL-fast, CR-fed, CR-fast) were analyzed by real-time RT–PCR. All data were normalized to *Tbp* expression (n = 5–6). Values are mean ± SEM. *: $p < 0.05$, **: $p < 0.01$, ***: $p < 0.001$ vs. AL, $: $p < 0.05$, $$: $p < 0.01$, $$$: $p < 0.001$ vs. fed, analyzed by Tukey's test after 2-way ANOVA.

(rWAT and eWAT) and sWAT, but that there are not large differences in FA synthesis among the depots.

3.4. Insulin signaling in the three white adipose tissue depots

The phosphorylation of HSL is negatively regulated by insulin signaling (Berwick et al., 2002; Lampidonis et al., 2011). To investigate the regulatory mechanisms underlying the CR-associated increase in lipolytic activity, we measured the abundance of total IRS and pAKT proteins, which are indicative of the degree of activation of insulin signaling, in the three WAT depots. Total IRS1 was detectable in sWAT, but barely detectable in rWAT and eWAT. Interestingly, CR shifted the bands of total IRS1 to a higher molecular weight in sWAT of fed rats (Fig. S3A–C). In rWAT and eWAT, CR did not change the abundance of either pAKT or total AKT under fed conditions (Fig. 5A, B, D, E, G, H). However, in sWAT, CR decreased total AKT abundance, and tended to increase pAKT abundance, resulting in a CR-associated upregulation of the pAKT to total AKT ratio (Fig. 5C, F, I, L). In all three WAT depots, CR exaggerated the difference in the pAKT to total AKT ratio between fed and fasted conditions (Fig. 5J–L). These findings suggest that CR improves the switching of AKT activity between fed and fasted conditions, regardless of the lower abundance of total AKT that was observed, particularly in sWAT. In addition, to evaluate CR effects on circulating glucose and insulin, we measured plasma glucose and insulin levels in the four groups. Plasma glucose levels were significantly lower in CR-fed than AL-fed rats, but showed no difference between fasting and fed conditions (Table 1). In contrast, plasma insulin levels were not significantly different between AL and CR rats, but were significantly lower in fasting than fed conditions (Table 1). These data may reflect a CR-associated improvement in insulin signaling activity.

3.5. Expression of adipocytokines and macrophage markers in the three WAT depots

To further investigate the differences in phenotype among the WAT depots, we measured the mRNA expression levels of adipocytokines. CR markedly increased *adiponectin* mRNA expression in sWAT and tended to increase *adiponectin* expression in eWAT, but had no effect in rWAT. However, fasting significantly and similarly downregulated *adiponectin* mRNA expression in all three WAT depots of CR rats (Fig. 6A–C). In addition, we measured plasma high molecular weight adiponectin levels. Plasma adiponectin levels were higher in CR rats than AL rats, particularly in fasted conditions (Table 1). CR markedly downregulated *leptin* mRNA expression in rWAT and eWAT, but had no effect in sWAT. In contrast, fasting significantly downregulated *leptin* mRNA expression in all three WAT depots of both AL and CR rats (Fig. 6D–F). These data suggest that the effects of CR on adipocytokine expression may differ between vWAT (rWAT and eWAT) and sWAT.

Moreover, we examined CR-associated changes in macrophage infiltration into adipose tissue. In all WAT depots, CR markedly and similarly downregulated mRNA expression of *Cd11c*, an M1 macrophage-specific marker (also known as integrin alpha X) (Fig. 7D–F). However, expression of *Cd163*, an M2 macrophage-specific marker, in CR rats was lower than that of AL rats in rWAT and sWAT, but not in eWAT (Fig. 7G–I). In addition, the CR-associated reduction in *F4/80* expression, a marker of all macrophages, was significant in rWAT and sWAT, but not in eWAT (Fig. 7A–C). Finally, we analyzed mRNA levels of representative inflammatory cytokines, *IL-6* and *Tnfα*. CR reduced *IL-6* mRNA expression in rWAT and eWAT, but not in sWAT (Fig. 7J–L). Conversely, *Tnfα* mRNA expression showed no notable differences in the three WAT depots (Fig. 7M–O).

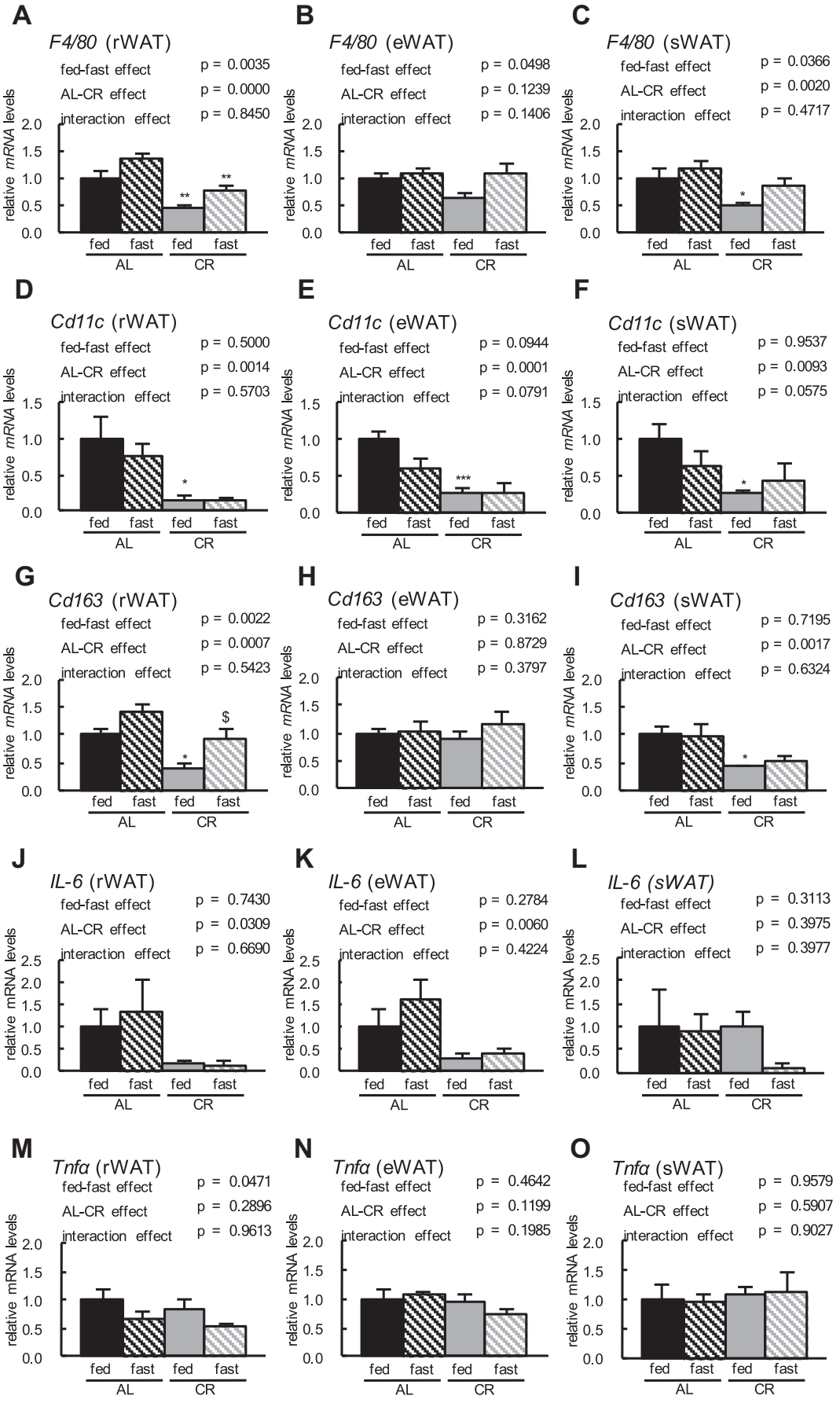

(caption on next page)

Fig. 7. Expression of macrophage and inflammation genes in rWAT, eWAT and sWAT
mRNA expression of the macrophage genes *F4/80* (A–C), *Cd11c* (D–F), and *Cd163* (G–I), in rWAT, eWAT and sWAT from the four groups (AL-fed, AL-fast, CR-fed, CR-fast) was analyzed by real-time RT–PCR. mRNA expression of the inflammation genes *IL-6* (J–L) and *Tnfα* (M–O), in rWAT, eWAT and sWAT from the four groups was analyzed by real-time RT–PCR. All data were normalized to *Tbp* expression (n = 5–6). Values are mean ± SEM. *: $p < 0.05$, **: $p < 0.01$, ***: $p < 0.001$ vs. AL, $: $p < 0.05$, $$: $p < 0.01$, $$$: $p < 0.001$ vs. fed, analyzed by Tukey's test after 2-way ANOVA.

4. Discussion

In this study, we demonstrate a differential response to CR among the retroperitoneal, epididymal and subcutaneous WAT depots. As shown in Table 1, CR preferentially affects WAT mass rather than that of other tissues, and the mass reduction was more significant in rWAT than in eWAT or sWAT. This finding was corroborated by CT analysis showing that CR predominantly reduced WAT mass in the upper abdomen. Moreover, the CR-associated reductions in WAT mass may reflect the presence of smaller adipocytes. In our AL rats, the rWAT adipocytes were larger than those in other WAT depots, consistent with previous reports (Mårin et al., 1992; Misra and Vikram, 2003). These larger rWAT adipocytes might thus be more susceptible to CR-induced mass reductions than the adipocytes in other depots.

Because adipocyte size is dependent on cellular TG content, we explored the influence of CR on lipid metabolism, especially lipogenesis and lipolysis, in the three WAT depots. In agreement with our previous study showing that CR enhances FA biosynthesis in eWAT (Okita et al., 2015), CR markedly and similarly upregulated the expression of lipogenic proteins in rWAT and sWAT, as well as in eWAT, under fed conditions (Fig. 3). In our previous report, we demonstrated that CR enhances mitochondrial biogenesis (Fujii et al., 2017). To compare this CR effect in rWAT, eWAT and sWAT, we measured the expression of proteins involved in mitochondria, including SIRT3, TOM20 and COXIV. The results showed that CR increased the abundance of these proteins in all three WAT depots of rats (Fig. S2). It is well known that HSL phosphorylation is negatively regulated by insulin signaling (AKT) and positively regulated by adrenergic signaling (protein kinase A) (Ramakrishna and Benjamin, 1985; Potapova et al., 2000; Holm, 2003; Lampidonis et al., 2011). Differences in AKT phosphorylation are indicative of differences in insulin sensitivity (Wojtaszewski et al., 2000) and it is widely accepted that CR enhances insulin sensitivity. Therefore, we predicted that CR would exaggerate the difference in AKT phosphorylation between the fed and fasted states. As expected, in all three WAT depots but particularly in sWAT, the difference in AKT phosphorylation between the fed and fasted states was greater for CR rats. However, the pHSL/HSL ratio did not appear to be negatively correlated with the pAKT/AKT ratio in rWAT or eWAT of CR rats, suggesting that insulin-stimulated HSL activation might not be involved in the lipolysis observed in rWAT or eWAT of CR rats.

β-adrenergic signaling leads to the intracellular accumulation of cyclic adenosine monophosphate and subsequent protein kinase A-mediated phosphorylation of HSL, thereby inducing lipolysis (Carmen and Victor, 2006; Jocken and Blaak, 2008). Because pHSL/HSL was significantly upregulated under fed conditions and downregulated under fasting conditions in rWAT and eWAT of CR rats, we consider that the CR-associated HSL activation may likewise not be regulated by insulin signaling. Conversely, pAKT/AKT was markedly lower, and pHSL/HSL was higher, during fasting in sWAT of CR rats. Therefore, insulin signaling might regulate fasting-associated lipolysis in sWAT of CR rats. To evaluate more directly insulin signaling, we examined total IRS1 protein levels. CR shifted total IRS1 bands to higher molecular weight in only sWAT of fed rats. Interestingly, previous articles showed that the bands of total IRS1 in insulin-treated cells were slightly shifted to high molecular weight (Sun et al., 1992; Pederson et al., 2001). These findings probably suggest that the CR-associated shift of total IRS-1 bands may reflect activation of insulin signaling predominantly in sWAT. It has been reported that insulin signaling negatively regulates ATGL mRNA (Kim et al., 2006). Because CR upregulated the expression of ATGL in fasted CR rats, ATGL might regulate the CR-enhanced lipolysis through altered insulin signaling during fasting.

It has been shown previously that three months of CR from 5 months of age lowered mRNA expression of *Cd11c* and *arginase-1*, M2 macrophage-specific markers, in eWAT, but not rWAT or sWAT, of rats (Rojas et al., 2016). In contrast to these findings, our data show that CR reduced *Cd11c* expression in all three WAT depots, and *Cd163* expression in rWAT and sWAT only. Previously, we reported that 4.5–5.5 months of CR from 6 weeks of age downregulated the mRNA expression of *F4/80* and *Cd11c*, but did not affect that of *Cd163* (Chujo et al., 2013), and the data presented herein are consistent with these observations. The reason for the discrepancy between our studies and others may be differences in experimental conditions, including the duration and timing of CR. In mice, CR had similar effects on vWAT and sWAT, downregulating M1 macrophage markers and upregulating M2 macrophage markers (Fabbiano et al., 2016). Promotion of M2 macrophage proliferation is known to be associated with the trans-differentiation of white adipocytes into brown-like adipocytes ("browning") in sWAT (Hui et al., 2015). However, despite reports that CR induces browning in mice, we did not observe multilocular lipid droplets (the main adipocyte phenotype in browning WAT) in sWAT of CR rats (Fig. 2A) (Fabbiano et al., 2016). Based on this observation, we assumed that browning of sWAT might occur to a lesser extent in rats than in mice. The differences between rats and mice in M2 macrophage infiltration and/or sensitivity of adipocyte browning to M2 macrophages might explain the differences observed in sWAT browning between these two species. In our analysis, CR tended to reduced *IL-6* mRNA expression, partially in accordance with *Cd11c* mRNA expression, but, unexpectedly, did not impact on *Tnfα* mRNA expression in any of the three WAT depots. This result suggests that severe inflammation does not occur in the WAT of AL rats, despite certain infiltration of M1 macrophages. Moreover, in sWAT of fed rats, CR did not reduce *IL-6* mRNA expression. This may be due to the smaller inflammatory reaction that accompanies aging in sWAT (Rojas et al., 2016).

In the present study, we analyzed the response of rWAT, eWAT, and sWAT to CR. We show that CR differentially affects the morphology and characteristics of these depots, including adipocyte size, lipid metabolism, insulin signaling, adipocytokine profile and macrophage infiltration. Therefore, we propose that it is important to evaluate the effects of CR on WAT using several parameters and in various WAT depots.

Acknowledgements

We thank all members of the Departments of Molecular Pathology and Metabolic Disease, and the Animal Center, of the Faculty of Pharmaceutical Sciences, Tokyo University of Science, for their assistance. We thank Alice Tait, PhD, from Edanz Group (www.edanzediting.com/ac) for editing a draft of this manuscript.

Funding sources

This work was partially supported by Grants-in-Aid for Scientific Research (C) (No. 19590396) and for Challenging Exploratory Research (No. 26670193) from the Japan Society for the Promotion of Science, and by the MEXT-supported program for Strategic Research at Private Universities, 2014–2018.

Appendix A. Supplementary data

Supplementary data to this article can be found online at https://doi.org/10.1016/j.exger.2018.01.016.

References

Berwick, D.C., Hers, I., Heesom, K.J., Moule, S.K., Tavaré, J.M., 2002. The identification of ATP-citrate lyase as a protein kinase B (Akt) substrate in primary adipocytes. J. Biol. Chem. 277, 33895–33900.

Bruss, M.D., Khambatta, C.F., Ruby, M.A., Aggarwal, I., Hellerstein, M.K., 2010. Calorie restriction increases fatty acid synthesis and whole body fat oxidation rates. Am. J. Physiol. Endocrinol. Metab. 298, E108–E116.

Carmen, G.Y., Victor, S.M., 2006. Signalling mechanisms regulating lipolysis. Cell. Signal. 18, 401–408.

Chujo, Y., Fujii, N., Okita, N., Konishi, T., Narita, T., Yamada, A., Haruyama, Y., Tashiro, K., Chiba, T., Shimokawa, I., Higami, Y., 2013. Caloric restriction-associated remodeling of rat white adipose tissue: effects on the growth hormone/insulin-like growth factor-1 axis, sterol regulatory element binding protein-1, and macrophage infiltration. Age (Dordr.) 35, 1143–1156.

DeClercq, V., Taylor, C., Zahradka, P., 2008. Adipose tissue: the link between obesity and cardiovascular disease. Cardiovasc. Hematol. Disord. Drug Targets 8, 228–237.

Engfeldt, P., Arner, P., 1988. Lipolysis in human adipocytes, effects of cell size, age and of regional differences. Horm. Metab. Res. Suppl. 19, 26–29.

Fabbiano, S., Suárez-Zamorano, N., Rigo, D., Veyrat-Durebex, C., Dokic, A.S., Colin, D.J., Trajkovski, M., 2016. Caloric restriction leads to browning of white adipose tissue through type 2 immune signaling. Cell Metab. 24, 434–446.

Fisher, F.M., McTernan, P.G., Valsamakis, G., Chetty, R., Harte, A.L., Anwar, A.J., Starcynski, J., Crocker, J., Barnett, A.H., McTernan, C.L., Kumar, S., 2002. Differences in adiponectin protein expression: effect of fat depots and type 2 diabetic status. Horm. Metab. Res. 34, 650–654.

Fujii, N., Narita, T., Okita, N., Kobayashi, M., Furuta, Y., Chujo, Y., Sakai, M., Yamada, A., Takeda, K., Konishi, T., Sudo, Y., Shimokawa, I., Higami, Y., 2017. Sterol regulatory element-binding protein-1c orchestrates metabolic remodeling of white adipose tissue by caloric restriction. Aging Cell 16, 508–517.

Holm, C., 2003. Molecular mechanisms regulating hormone-sensitive lipase and lipolysis. Biochem. Soc. Trans. 31, 1120–1124.

Hui, X., Gu, P., Zhang, J., Nie, T., Pan, Y., Wu, D., Feng, T., Zhong, C., Wang, Y., Lam, K.S.L., Xu, A., 2015. Adiponectin enhances cold-induced browning of subcutaneous adipose tissue via promoting M2 macrophage proliferation. Cell Metab. 22, 279–290.

Jocken, J.W., Blaak, E.E., 2008. Catecholamine-induced lipolysis in adipose tissue and skeletal muscle in obesity. Physiol. Behav. 94, 219–230.

Kim, J.Y., Tillison, K., Lee, J.H., Rearick, D.A., Smas, C.M., 2006. The adipose tissue triglyceride lipase ATGL/PNPLA2 is downregulated by insulin and TNF-α in 3T3-L1 adipocytes and is a target for transactivation by PPARγ. Am. J. Physiol. Endocrinol. Metab. 291, E115–E127.

Lampidonis, A.D., Rogdakis, E., Voutsinas, G.E., Stravopodis, D.J., 2011. The resurgence of hormone-sensitive lipase (HSL) in mammalian lipolysis. Gene 477, 1–11.

Mårin, P., Andersson, B., Ottosson, M., Olbe, L., Chowdhury, B., Kvist, H., Holm, G., Sjöström, L., Björntorp, P., 1992. The morphology and metabolism of intraabdominal adipose tissue in men. Metabolism 41, 1242–1248.

Misra, A., Vikram, N.K., 2003. Clinical and pathophysiological consequences of abdominal adiposity and abdominal adipose tissue depots. Nutrition 19, 457–466.

Okita, N., Hayashida, Y., Kojima, Y., Fukushima, M., Yuguchi, K., Mikami, K., Yamauchi, A., Watanabe, K., Noguchi, M., Nakamura, M., Toda, T., Higami, Y., 2012. Differential responses of white adipose tissue and brown adipose tissue to caloric restriction in rats. Mech. Ageing Dev. 133, 255–266.

Okita, N., Tsuchiya, T., Fukushima, M., Itakura, K., Yuguchi, K., Narita, T., Hashizume, Y., Sudo, Y., Chiba, T., Shimokawa, I., Higami, Y., 2015. Chronological analysis of caloric restriction-induced alteration of fatty acid biosynthesis in white adipose tissue of rats. Exp. Gerontol. 63, 59–66.

Ouchi, N., Parker, J.L., Lugus, J.J., Walsh, K., 2011. Adipokines in inflammation and metabolic disease. Nat. Rev. Immunol. 11, 85–97.

Pederson, T.M., Kramer, D.L., Rondinone, C.M., 2001. Serine/threonine phosphorylation of IRS-1 triggers its degradation: possible regulation by tyrosine phosphorylation. Diabetes 50, 24–31.

Potapova, I.A., El-Maghrabi, M.R., Doronin, S.V., Benjamin, W.B., 2000. Phosphorylation of recombinant human ATP: citrate lyase by cAMP-dependent protein kinase abolishes homotropic allosteric regulation of the enzyme by citrate and increases the enzyme activity. Allosteric activation of ATP: citrate lyase by phosphorylated sugars. Biochemistry 39, 1169–1179.

Ramakrishna, S., Benjamin, W.B., 1985. Cyclic nucleotide-independent protein kinase from rat liver. Purification and characterization of a multifunctional protein kinase. J. Biol. Chem. 260, 12280–12286.

Rojas, J.X.S., García-San Frutos, M., Horrillo, D., Lauzurica, N., Oliveros, E., Carrascosa, J.M., Fernández-Agulló, T., Ros, M., 2016. Differential development of inflammation and insulin resistance in different adipose tissue depots along aging in Wistar rats: effects of caloric restriction. J. Gerontol. A Biol. Sci. Med. Sci. 71, 310–322.

Strable, M.S., Ntambi, J.M., 2010. Genetic control of de novo lipogenesis: role in diet-induced obesity. Crit. Rev. Biochem. Mol. Biol. 45, 199–214.

Sun, X.J., Miralpeix, M., Myers, M.G., Glasheen, E.M., Backer, J.M., Kahn, C.R., White, M.F., 1992. Expression and function of IRS-1 in insulin signal transmission. J. Biol. Chem. 267, 22662–22672.

Torres-Leal, F.L., Fonseca-Alaniz, M.H., Rogero, M.M., Tirapegui, J., 2010. The role of inflamed adipose tissue in the insulin resistance. Cell Biochem. Funct. 28, 623–631.

Tran, T.T., Yamamoto, Y., Gesta, S., Kahn, C.R., 2008. Beneficial effects of subcutaneous fat transplantation on metabolism. Cell Metab. 7, 410–420.

Wojtaszewski, J.F., Hansen, B.F., Kiens, B., Markuns, J.F., Goodyear, L.J., Richter, E.A., 2000. Insulin signaling and insulin sensitivity after exercise in human skeletal muscle. Diabetes 49, 325–331.